

Attempt frequency of magnetization in nanomagnets with thin-film geometry

Hong-Ju Suh,¹ Changehoon Heo,¹ Chun-Yeol You,² Woojin Kim,³
Taek-Dong Lee,³ and Kyung-Jin Lee^{1,*}

¹*Department of Materials Science and Engineering, Korea University, Seoul 136-701, Korea*

²*Department of Physics, Inha University, Incheon 402-751, Korea*

³*Department of Materials Science and Engineering, KAIST, Daejeon 305-701, Korea*

(Received 27 March 2008; revised manuscript received 29 June 2008; published 29 August 2008)

Solving the stochastic Landau-Lifshitz-Gilbert equation numerically, we investigate the effect of the potential landscape on the attempt frequency of magnetization in nanomagnets with the thin-film geometry. Numerical estimates of the attempt frequency are analyzed in comparison with theoretical predictions from the Fokker-Planck equation for the Néel-Brown model. It is found that for a nanomagnet with the thin-film geometry, theoretically predicted values for the universal case are in excellent agreement with numerical estimates.

DOI: [10.1103/PhysRevB.78.064430](https://doi.org/10.1103/PhysRevB.78.064430)

PACS number(s): 75.60.Lr, 72.25.Ba, 85.75.-d

I. INTRODUCTION

Much effort has been expended in fabricating deep sub-micron patterned magnets with the thin-film geometry. From the scientific point of view, such a small magnet is a good model system to study basic magnetism via a direct comparison with an idealized theoretical prediction. From the application point of view, a steady progress of the patterning technology for fabricating a smaller cell has led to magnetic devices such as spin-valve read sensors for the hard disk drive and magnetic random access memories (MRAMs) utilizing the spin-transfer torque^{1,2} (STT) into a higher density, i.e., a smaller magnetic volume.

Thermal agitation of a magnetization becomes more and more important as the magnetic volume of a unit cell decreases. In the spin-valve read sensor, the so-called “magnoise” is a manifestation of the thermally excited ferromagnetic resonance in the sensor stack.^{3,4} In the STT-MRAM, thermal agitation hinders a continuous miniaturization of the device because it can cause spontaneous changes of magnetization direction from one stable state to another.

Thermal relaxation time is a statistical time scale for which a magnetization escapes from an initial local minimum state over an energy barrier. The thermal relaxation time τ of a magnetization is described by the Néel-Brown model^{5,6} in the high energy barrier asymptote $\tau = f_0^{-1} \exp[U_B/k_B T]$, where f_0 is the attempt frequency, U_B is the energy barrier measuring the difference between a local minimum and a saddle point, k_B is the Boltzmann constant, and T is the temperature in Kelvin.

Experimental studies on the thermal relaxation of magnetization generally assume a constant attempt frequency.⁷⁻⁹ However, Brown showed theoretically that the attempt frequency is not constant but depends on many parameters such as the damping constant and the magnetic properties.⁶ Followed by Brown’s initial work,⁶ theoretical formulae of the attempt frequency for different potential symmetry were proposed.¹⁰⁻¹⁷

Accurate theoretical formulae of the attempt frequency are necessary for modeling experiments and predicting quantitatively the superparamagnetic limit for device applications.

However, it is not easy to experimentally verify the theoretical formulae because (i) an experimentally measurable quantity such as the switching field is mostly governed by the energy barrier, not by the attempt frequency, and (ii) the damping constant, a key factor affecting the attempt frequency, of a small magnet is not definite in general.^{18,19}

In this work, by means of a numerical study based on the stochastic Landau-Lifshitz-Gilbert (LLG) equation,^{6,20} we investigate the validity of the proposed theoretical formulae. It is found that for a nanomagnet with the thin-film geometry, theoretically predicted values for the universal case are in excellent agreement with numerical estimates whereas theoretical values for the intermediate-to-high damping limit and the very low damping limit fail to reproduce numerical ones in practically meaningful ranges of the damping constant.

This paper is organized as follows: After introducing the proposed theoretical formulae (Sec. II) and numerical model used in this work (Sec. III), we show in Sec. IV the effect of the shape anisotropy, i.e., potential landscape, on the attempt frequency for various damping constants and discuss about validity of the theoretical formulae by comparing with numerical estimates. In Sec V, we summarize this work.

II. THEORETICAL FORMULAE OF THE ATTEMPT FREQUENCY

The magnetic potential U of a single-domain particle with uniaxial symmetry in the presence of a static external longitudinal field H is given by

$$\begin{aligned} U &= K_U(1 - \alpha_1^2) - M_S H \alpha_1 + \frac{1}{2}(N_1 \alpha_1^2 + N_2 \alpha_2^2 + N_3 \alpha_3^2) M_S^2 \\ &= K_U(1 - \sin^2 \vartheta \cos^2 \varphi) - M_S H \sin \vartheta \cos \varphi \\ &\quad + \frac{1}{2}(N_1 \sin^2 \vartheta \cos^2 \varphi + N_2 \sin^2 \vartheta \sin^2 \varphi \\ &\quad + N_3 \cos^2 \vartheta) M_S^2, \end{aligned} \quad (1)$$

where K_U is the uniaxial anisotropy, M_S is the saturation magnetization, H is the external field applied along the magnetic easy axis, ϑ and φ are the polar angle of magnetization

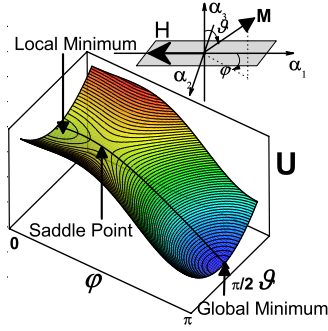


FIG. 1. (Color online) Magnetic potential surface of a single-domain particle with nonaxial symmetry. α_1 is the magnetic easy axis and the external field H is applied along the easy axis. The magnetic energy U in Eq. (1) has two equivalent saddle points and two minima points: local minimum and global minimum. In thermally activated switching, the magnetization changes from local minimum to global minimum passing through saddle point.

vector and the azimuthal angle of magnetization vector, respectively, α_i ($i=1,2,3$) is the direction cosines of magnetization vector, and N_i is the demagnetization factor along α_i axis (Fig. 1).

In an axially symmetric potential [$U(\vartheta, \varphi) = U(\vartheta)$], Brown⁶ showed the attempt frequency is not a constant, but a complex function as

$$f_0 = \frac{\gamma\alpha}{1 + \alpha^2} \sqrt{\frac{H_K^3 M_S V}{2\pi k_B T}} (1 - h^2)(1 + h), \quad (2)$$

where γ is the gyromagnetic ratio, α is the damping constant, H_K is the effective anisotropy field, V is the magnetic volume, h is H/H_K , and H is the external field applied along the magnetic easy axis.

Dependence of the attempt frequency on the damping constant for a nonaxially symmetric potential was first theoretically predicted for two limiting cases: (i) intermediate-to-high damping (IHD) case¹⁰ and (ii) very low damping (VLD) case.^{11,12} Later, the universal theoretical equation^{13–17} which is valid for all values of the damping constant was derived by extending the Meshkov-Mel'nikov depopulation factor to the magnetic case.²¹ In this work, numerical estimates of the attempt frequencies are compared with the theories for the two limiting cases and the universal one.

In the IHD limit, the attempt frequency for a nonaxially symmetric potential is given as¹⁰

$$f_0^{\text{IHD}} = \frac{\gamma\alpha\sqrt{c_{m1}c_{m2}}}{4\pi M_S(1 + \alpha^2)} \frac{(c'_2 - c_1) + \sqrt{(c_1 + c'_2)^2 + 4c_1c'_2/\alpha^2}}{\sqrt{c_1c'_2}}, \quad (3)$$

where c_{m1} and c_{m2} are the coefficients in the expansion of magnetic potential U about a local energy minimum for the initial magnetic state $U = U_m + 1/2(c_{m1}\alpha_1^2 + c_{m2}\alpha_2^2) + \dots$, and c_1 and c'_2 are the coefficients in the expansion about the saddle point $U = U_S + 1/2(c_1\alpha_1^2 - c'_2\alpha_2^2) + \dots$, respectively.

Klik and Gunther¹¹ and Coffey *et al.*¹² derived a theoretical formalism of the attempt frequency for a nonaxially symmetric potential in the VLD limit as

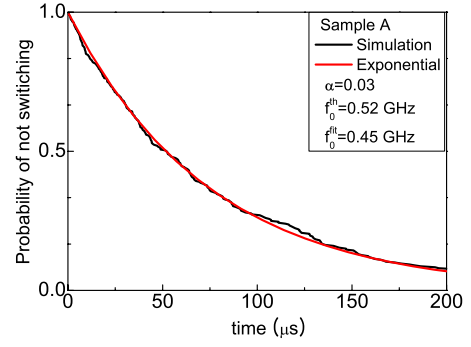


FIG. 2. (Color online) Probability of not switching ($1 - P_{\text{SW}}$) versus magnetization switching time at $\alpha=0.03$ in sample A ($l \times w \times d = 21 \times 20 \times 20$ nm³).

$$f_0^{\text{VLD}} = \frac{\gamma\alpha\sqrt{c_{m1}c_{m2}}}{2\pi M_S(1 + \alpha^2)} S, \quad (4)$$

where S is the dimensionless action variable at the saddle-point potential U_S defined as

$$S = \frac{V}{k_B T} \oint_{U(\vartheta, \varphi) = U_S} \left[(1 - \cos^2 \vartheta) \frac{\partial}{\partial \cos \vartheta} U(\vartheta, \varphi) d\varphi - \frac{1}{(1 - \cos^2 \vartheta)} \frac{\partial}{\partial \varphi} U(\vartheta, \varphi) d \cos \vartheta \right]. \quad (5)$$

For the universal case, the attempt frequency is given by^{13–17}

$$f_0 = A(\alpha S) f_0^{\text{IHD}}, \quad (6)$$

where S is given by Eq. (5).

$A(\alpha S)$ is a factor which interpolates between the VLD and IHD limits and given by

$$A(\alpha S) = \exp \left[\frac{1}{\pi} \int_0^\infty \frac{\ln[1 - \exp\{-\alpha S(\lambda^2 + 1/4)\}]}{\lambda^2 + 1/4} d\lambda \right]. \quad (7)$$

III. NUMERICAL MODEL

We performed macrospin calculations by means of the stochastic LLG equation

$$\frac{\partial \mathbf{M}}{\partial t} = -\gamma \mathbf{M} \times \mathbf{H}_{\text{eff}} + \frac{\alpha}{M_S} \frac{\partial \mathbf{M}}{\partial t}, \quad (8)$$

where \mathbf{M} is the magnetization vector and \mathbf{H}_{eff} is the effective magnetic field including the external, the magnetostatic, and the thermal fluctuation. To estimate the thermal relaxation time τ , we used a macrospin model with $U_B/k_B T$ of about 10 because of excessive computation time. Probability of switching P_{SW} of thermally activated switching was estimated by counting the number of successful switching out of 500 switching events. The attempt frequency is obtained by fitting numerical results of P_{SW} as a function of the time using the Arrhenius-Néel decay of the probability of switching $P_{\text{SW}} = 1 - \exp[-f_0 t \exp(-U_B/k_B T)]$ as shown in Fig. 2.

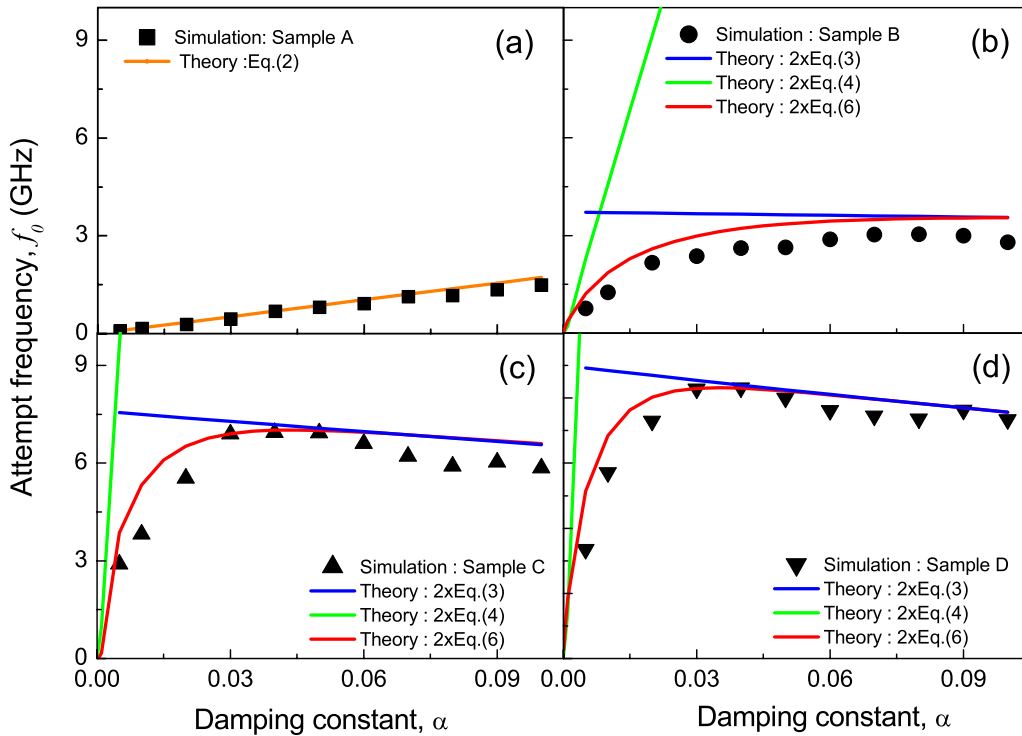


FIG. 3. (Color online) (a), (b), (c), and (d) show the attempt frequency as a function of the damping constant α for samples A, B, C, and D, respectively. Solid lines are theoretically predicted values and symbols are numerical results. Dimensions of samples and parameters are given in the text ($M_S=800$ emu/cm³).

IV. EFFECT OF SHAPE ANISOTROPY ON THE ATTEMPT FREQUENCY

We have calculated attempt frequencies of various sized nanomagnets; sample A ($l \times w \times d = 21 \times 20 \times 20$ nm³), sample B ($25 \times 21 \times 16$ nm³), sample C ($40 \times 30 \times 7$ nm³), and sample D ($100 \times 28 \times 3$ nm³), where l (length), w (width), and d (thickness) are the sample dimensions along x , y , and z axes, respectively, and thus the x axis is the easy axis. For all four samples, constant values of volume $V (=8400$ nm³), effective in-plane anisotropy $H_K (=875.4$ Oe), and external field $H (= -540$ Oe) were used to exclude their effects on the attempt frequency. The thermal stability factor $U_B/k_B T$ was 10.425, a good number for the high energy barrier approximation. The magnetic potential U of sample A is axially symmetric since $w=d$, whereas U of other samples are nonaxially symmetric since $w \neq d$.

The numerical results of the attempt frequency for the nanomagnet with an axially symmetric potential (sample A) are shown in Fig. 3(a). To our knowledge, Eq. (2) was tested once by adopting the same way used in this work,²² and it was reported that the theoretical value of attempt frequency is different from the numerically estimated value by an order of magnitude. This inconsistency may have prevented further numerical studies on the attempt frequency. However, we found excellent agreement between Eq. (2) and numerically estimated values [see Fig. 3(a)]. The difference between the result in the Ref. 22 and ours originates from the sign of h in Eq. (2). h should be negative since the magnetization is initially in a shallower local energy minimum, whereas it was assumed to be positive in the Ref. 22. The excellent agree-

ment verifies the validity of our numerical approach to estimate the attempt frequency in this work.

Figures 3(b)–3(d) show the dependence of the attempt frequency on the damping constant for the samples B, C, and D, respectively. Two features are worth mentioning. First, the attempt frequency increases with increasing w/d . For instance, the attempt frequency of sample D is an order of magnitude higher than that of sample A in the wide range of damping constant (Fig. 3). Second, when the potential landscape is nonaxially symmetric, there are two regimes of the damping constant where the attempt frequency shows an explicitly different dependence on the damping constant. At low damping ($\alpha < 0.03$), the attempt frequency increases with the damping constant whereas at high damping ($\alpha > 0.03$), it slightly decreases.

Considering the increase of attempt frequency with w/d , it should be noted that both Eqs. (3) and (4) contain $\sqrt{c_{m1}c_{m2}}$ which is an averaged curvature of potential at the local minimum. Other terms do not vary much with w/d . The c_{m1} is given by $H_K M_S (1+h)$ which is a constant for all four samples since both effective in-plane anisotropy field H_K and external field H are assumed to be constants. The c_{m2} is given by $H_K M_S (1+h + \frac{(N_3 - N_2)M_S}{H_K})$, where N_2 (N_3) is the demagnetization factor along the in-plane hard (out-of-plane hard) axis. The c_{m2} significantly varies with the sample shape since $\frac{(N_3 - N_2)M_S}{H_K}$ term is dominant. Therefore, an important parameter to determine the attempt frequency is the coefficient c_{m2} which measures the curvature of potential along the direction cosine α_2 and is related to the out-of-plane demagnetization effect. A larger curvature of potential at a local mini-

mum results in a higher attempt frequency. It is because the magnetization moving away from a local minimum due to a thermal random force experiences an instantaneous restoring force proportional to the curvature. The curvature c_{m2} becomes smaller and smaller as the aspect ratio of sample w/d approaches the unity. Among the tested samples, sample D provides the largest c_{m2} and thus, the highest attempt frequency.

In order to understand dependence of the attempt frequency on the damping constant, we compare numerical results with the theoretical formulae [Eq. (3) (IHD), Eq. (4) (VLD), and Eq. (6) (universal)] from the Fokker-Planck equation for the Néel-Brown model. In the whole range of damping constant, the numerical results are in good agreements with Eq. (6) multiplied by factor 2. The equations were derived for the escape of magnetization over only one shallower barrier assuming different barrier heights between in-plane clockwise switching and counter clockwise one. In our case, the two energy barriers are identical since no symmetry breaking exists, validating the multiplication by factor 2.

The theoretical values obtained from Eq. (3) (IHD) partially coincide with the numerical results in high damping regime ($\alpha > 0.04$), whereas Eq. (4) (VLD) predicts much higher attempt frequencies than the numerical results in the tested range of damping constant ($0.005 < \alpha < 0.1$).

In the VLD, the escape rate is evaluated from the energy loss per cycle of a particle on the escape rate trajectory.^{15,17} The assumption made in deriving Eq. (4), replacing the energy loss per cycle of the almost periodic motion at the barrier energy by the barrier height, is necessarily crude and only applies when the damping constant is less than about 0.001. The failure of Eq. (4) to estimate the attempt frequency is also found in Ref. 14 where comparisons among the IHD escape rates, the VLD escape rates, the universal solution based on the Meshkov-Mel'nikov depopulation factor, and the exact escape rate based on the continued fraction solution of the Fokker-Planck for the lowest eigenvalue were made. In Ref. 14, it is shown that the VLD asymptote begins

to fail for the damping constant of the order of 10^{-2} even if the action on the escape trajectory is evaluated exactly whereas the universal solution provides a reasonably accurate approximation throughout the whole range of damping.

Therefore, it is obvious that the universal escape rate [Eq. (6)] provides an accurate description of the behavior of the exact escape rate provided that the barrier height is sufficient to allow one to define an escape rate. Furthermore, since the damping constant in a typical nanomagnet with the thin-film geometry is in the range between 0.005 and 0.03 (Refs. 23–26) where the VLD and the IHD approximations show evidently wrong predictions for the attempt frequency, Eq. (6) should be used to design experiments and to interpret experimental results performed at nonzero temperatures.

V. SUMMARY

In a nanomagnet with the thin-film geometry, the demagnetization energy along the magnetic hard axis is a main factor affecting the attempt frequency. Comparing numerical estimates of the attempt frequency of magnetization with the theoretically predicted values, we verify the validity of the theoretical formula of the attempt frequency for the universal case. However, the theoretical formulae in the low damping limit and the intermediate-high damping limit fail to reproduce numerical values for the typical range of the damping constant. Therefore, the attempt frequency obtained from the theoretical equation for the universal case should be used to design experiments and to interpret experimental results performed at nonzero temperatures.

ACKNOWLEDGMENTS

Comments by Hyun-Woo Lee and Sug-Bong Choe are appreciated. This work is supported by the Korea Science and Engineering Foundation (KOSEF) through the Basic Research Program funded by the Ministry of Science and Technology (Contract No. R01-2007-000-20281-0) and Samsung Electronics.

*kj_lee@korea.ac.kr

¹J. C. Slonczewski, *J. Magn. Magn. Mater.* **159**, L1 (1996).

²L. Berger, *Phys. Rev. B* **54**, 9353 (1996).

³N. Smith and P. Arnett, *Appl. Phys. Lett.* **78**, 1448 (2001).

⁴J.-G. Zhu, *J. Appl. Phys.* **91**, 7273 (2002).

⁵L. Néel, *Ann. Geophys. (C.N.R.S.)* **5**, 99 (1949).

⁶W. F. Brown, Jr., *Phys. Rev.* **130**, 1677 (1963).

⁷W. Wernsdorfer, E. B. Orozco, K. Hasselbach, A. Benoit, B. Barbara, N. Demoncy, A. Loiseau, H. Pascard, and D. Mailly, *Phys. Rev. Lett.* **78**, 1791 (1997).

⁸N. D. Rizzo, T. J. Silva, and A. B. Kos, *Phys. Rev. Lett.* **83**, 4876 (1999).

⁹S. I. Woods, J. R. Kirtley, Shouheng Sun, and R. H. Koch, *Phys. Rev. Lett.* **87**, 137205 (2001).

¹⁰W. F. Brown, Jr., *IEEE Trans. Magn.* **15**, 1197 (1979).

¹¹I. Klik and L. Gunther, *J. Stat. Phys.* **60**, 473 (1990).

¹²W. T. Coffey, D. S. F. Crothers, J. L. Dormann, L. J. Geoghegan, and E. C. Kennedy, *Phys. Rev. B* **58**, 3249 (1998).

¹³W. T. Coffey, D. A. Garanin, and D. McCarthy, *Adv. Chem. Phys.* **117**, 528 (2001).

¹⁴P. M. Dèjardin, D. S. F. Crothers, W. T. Coffey, and D. J. McCarthy, *Phys. Rev. E* **63**, 021102 (2001).

¹⁵Y. P. Kalmykov, W. T. Coffey, and S. V. Titov, *Phys. Solid State* **47**, 272 (2005).

¹⁶D. A. Garanin, E. C. Kennedy, D. S. F. Crothers, and W. T. Coffey, *Phys. Rev. E* **60**, 6499 (1999).

¹⁷Y. P. Kalmykov, W. T. Coffey, B. Ouari, and S. V. Titov, *J. Magn. Magn. Mater.* **292**, 372 (2005).

¹⁸W. T. Coffey, D. S. F. Crothers, J. L. Dormann, Yu. P. Kalmykov, E. C. Kennedy, and W. Wernsdorfer, *Phys. Rev. Lett.* **80**, 5655 (1998).

¹⁹L. H. F. Andrade, A. Laraoui, M. Vomir, D. Muller, J. P. Sto-

- quert, C. Estournès, E. Beaupaire, and J. Y. Bigot, *Phys. Rev. Lett.* **97**, 127401 (2006).
- ²⁰R. W. Chantrell, J. D. Hannay, M. Wongsam, T. Schrefl, and H. J. Richter, *IEEE Trans. Magn.* **34**, 1839 (1998).
- ²¹V. I. Mel'nikov and S. V. Meshkov, *J. Chem. Phys.* **85**, 1018 (1986).
- ²²E. D. Boerner and H. N. Bertram, *IEEE Trans. Magn.* **34**, 1678 (1998).
- ²³I. N. Krivorotov, N. C. Emley, J. C. Sankey, S. I. Kiselev, D. C. Ralph, and R. A. Buhrman, *Science* **307**, 228 (2005).
- ²⁴J. C. Sankey, P. M. Braganca, A. G. F. Garcia, I. N. Krivorotov, R. A. Buhrman, and D. C. Ralph, *Phys. Rev. Lett.* **96**, 227601 (2006).
- ²⁵J. C. Sankey, Y.-T. Cui, J. Z. Sun, J. C. Slonczewski, R. A. Buhrman, and D. C. Ralph, *Nat. Phys.* **4**, 67 (2008).
- ²⁶H. Kubota, A. Fukushima, K. Yakushiji, T. Nagahama, S. Yuasa, K. Ando, H. Maehara, Y. Nagamine, K. Tsunekawa, D. D. Djayaprawira, N. Watanabe, and Y. Suzuki, *Nat. Phys.* **4**, 37 (2008).